



SaeR as a novel target for antivirulence therapy against *Staphylococcus aureus*

Peng Gao, Yuanxin Wei, Suying Hou, Pok-Man Lai, Han Liu, Sherlock Shing Chiu Tai, Victor Yat Man Tang, Pradeep Halebeedu Prakash, Kong-Hung Sze, Jonathan Hon Kwan Chen, Hongzhe Sun, Xuechen Li & Richard Yi-Tsun Kao

To cite this article: Peng Gao, Yuanxin Wei, Suying Hou, Pok-Man Lai, Han Liu, Sherlock Shing Chiu Tai, Victor Yat Man Tang, Pradeep Halebeedu Prakash, Kong-Hung Sze, Jonathan Hon Kwan Chen, Hongzhe Sun, Xuechen Li & Richard Yi-Tsun Kao (2023) SaeR as a novel target for antivirulence therapy against *Staphylococcus aureus*, *Emerging Microbes & Infections*, 12:2, 2254415, DOI: [10.1080/22221751.2023.2254415](https://doi.org/10.1080/22221751.2023.2254415)

To link to this article: <https://doi.org/10.1080/22221751.2023.2254415>



© 2023 The Author(s). Published by Informa UK Limited, trading as Taylor & Francis Group, on behalf of Shanghai Shangyixun Cultural Communication Co., Ltd



[View supplementary material](#)



Published online: 10 Sep 2023.



[Submit your article to this journal](#)



Article views: 1206











[View related articles](#)



[View Crossmark data](#)

SaeR as a novel target for antivirulence therapy against *Staphylococcus aureus*

Peng Gao ^a, Yuanxin Wei^a, Suying Hou^a, Pok-Man Lai^a, Han Liu ^b, Sherlock Shing Chiu Tai^a, Victor Yat Man Tang^a, Pradeep Halebeedu Prakash ^a, Kong-Hung Sze ^a, Jonathan Hon Kwan Chen ^a, Hongzhe Sun ^b, Xuechen Li ^b and Richard Yi-Tsun Kao ^a

^aDepartment of Microbiology, School of Clinical Medicine, Li Ka Shing Faculty of Medicine, The University of Hong Kong, Pokfulam, Hong Kong Special Administrative Region, China; ^bMorningside Laboratory for Chemical Biology and Department of Chemistry, The University of Hong Kong, Hong Kong, People's Republic of China

ABSTRACT

Staphylococcus aureus is a major human pathogen responsible for a wide range of clinical infections. SaeRS is one of the two-component systems in *S. aureus* that modulate multiple virulence factors. Although SaeR is required for *S. aureus* to develop an infection, inhibitors have not been reported. Using an *in vivo* knockdown method, we demonstrated that SaeR is targetable for the discovery of antivirulence agent. HR3744 was discovered through a high-throughput screening utilizing a GFP-Lux dual reporter system driven by saeP1 promoter. The antivirulence efficacy of HR3744 was tested using Western blot, Quantitative Polymerase Chain Reaction, leucotoxicity, and haemolysis tests. In electrophoresis mobility shift assay, HR3744 inhibited SaeR-DNA probe binding. WaterLOGSY-NMR test showed HR3744 directly interacted with SaeR's DNA-binding domain. When SaeR was deleted, HR3744 lost its antivirulence property, validating the target specificity. Virtual docking and mutagenesis were used to confirm the target's specificity. When Glu159 was changed to Asn, the bacteria developed resistance to HR3744. A structure–activity relationship study revealed that a molecule with a slight modification did not inhibit SaeR, indicating the selectivity of HR3744. Interestingly, we found that SAV13, an analogue of HR3744, was four times more potent than HR3744 and demonstrated identical antivirulence properties and target specificity. In a mouse bacteraemia model, both HR3744 and SAV13 exhibited *in vivo* effectiveness. Collectively, we identified the first SaeR inhibitor, which exhibited *in vitro* and *in vivo* antivirulence properties, and proved that SaeR could be a novel target for developing antivirulence drugs against *S. aureus* infections.

ARTICLE HISTORY Received 19 April 2023; Revised 27 August 2023; Accepted 28 August 2023




KEYWORDS *S. aureus*; SaeR; virulence; inhibitor; target


Introduction

The highly virulent nature of *Staphylococcus aureus* (*S. aureus*) makes it a life-threatening pathogen. It may invade any region of the body and produce symptoms ranging from moderately severe skin infections to fatal pneumonia and sepsis [1]. Methicillin-resistant *S. aureus* (MRSA) is a leading pathogen responsible for hospital- and community-acquired infections worldwide. Widely reported MRSA infections such as bacteraemia and skin and soft tissue infection pose a significant threat to patients. Limited therapeutic options are available to treat bacteria that are resistant to multiple classes of antibiotics, including vancomycin, β -lactams, and aminoglycosides [2]. In 2017, the World Health Organization (WHO) reported that antibiotics are becoming obsolete and highlighted that antimicrobial resistance is a global health and development threat. The rapid emergence

of resistant *S. aureus* strains especially for antibiotics like clindamycin, makes patients vulnerable to morbidity and mortality [3]. Meanwhile, antibiotics may exacerbate infections by enhancing bacterial virulence [4]. Additionally, antibiotics with its bacterial inhibition property, may generate selection pressure on pathogens leading to the emergence of resistant strains. Hence, the usage of antibiotics may not be an efficient and sustainable strategy to combat bacterial infections. There is an urgent need for an alternative anti-infective agent such as antivirulence molecules, which selectively inhibit the pathogenesis pathways, without inducing selective pressure in pathogens [5,6].

Multitude of virulence factors play a pivotal role in *S. aureus* pathogenesis. Infection starts with colonization which requires a diverse repertoire of virulence factors. Later, the bacteria disseminate by adapting

CONTACT Peng Gao  gaop0305@gmail.com; Richard Yi Tsun Kao  rytkao@hku.hk  Department of Microbiology, School of Clinical Medicine, Li Ka Shing Faculty of Medicine, The University of Hong Kong, 21 Sassoon Road, Pokfulam, Hong Kong Special Administrative Region, China

 Supplemental data for this article can be accessed online at <https://doi.org/10.1080/22221751.2023.2254415>.

© 2023 The Author(s). Published by Informa UK Limited, trading as Taylor & Francis Group, on behalf of Shanghai Shangyixun Cultural Communication Co., Ltd This is an Open Access article distributed under the terms of the Creative Commons Attribution-NonCommercial License (<http://creativecommons.org/licenses/by-nc/4.0/>), which permits unrestricted non-commercial use, distribution, and reproduction in any medium, provided the original work is properly cited. The terms on which this article has been published allow the posting of the Accepted Manuscript in a repository by the author(s) or with their consent.

to the host environment, subvert host functions, and finally evade the host immune response [7]. Blocking these infection pathways will make the pathogen more susceptible to the host immune system, leading to its natural clearance. Therefore, the utilization of antivirulence agents is crucial in attaining this goal, as they do not impose any selective pressure on the pathogens and may preserve the natural microbial flora within the host [8,9].

Voluminous literature on key regulatory networks in *S. aureus*, such as accessory gene regulator (*agrAC*), staphylococcal accessory regulator (*sarA*) and *S. aureus* exoprotein expression regulator (*saeRS*) has shown that these genes affect the expression of haemolysin A (*hla*) both *in vitro* and *in vivo*. Moreover, *sae* plays a crucial role in this context [10]. The histidine kinase (SaeS) and response regulator (SaeR) comprise a two-component system [11]. When exogenous stimuli (e.g., β -lactam antibiotics or α -defensin) are present, SaeS changes its conformation and auto-phosphorylates. The phosphate group is then transferred to SaeR. The binding of phosphorylated SaeR to the target gene promoter recruits RNA polymerase to the promoter, and initiates transcription [12].

Within the network, the *sae* system exerts its function as a central downstream regulator [13]. Many dominant virulence genes are controlled by the *sae* system, including *hly* (coding for β -haemolysin), *hla*, *cna* (coding for coagulase), *eap* (coding extracellular adherence protein), and *fnbA* (coding for fibronectin-binding protein A), probably by direct interactions with promoters of such genes [14]. Depending on the rate of *saeR* phosphorylation, *sae* system-controlled genes can be characterized into two distinct groups: class I and class II. A high level of phosphorylated SaeR (P-SaeR) is required for inducing class I target genes (e.g. the *sae* P1 promoter, *cna*, *fnbA*, and *eap*), whereas for class II targets (e.g. *hly* and *hla*), a basal level of P-SaeR is sufficient [15].

In a *saeRS* mutant, expression of exotoxin (*hla*, *pvl*) genes was decreased and the production of α -toxin was entirely abolished, leading to reduced haemolytic activity [14]. In a murine haematogenous pyelonephritis model, these properties, in turn, contributed to the reduced virulence of the *saeRS* mutant [16]. More importantly, mutation of *agr* or *sarA* was shown to have weak impact on the expression of *hla* *in vivo*. The deletion of *saeRS*, however, led to the repression of *hla* under *in vitro* and *in vivo* conditions [10].

In this study, our focus was to evaluate the targetability of SaeR and identify novel small molecules that can inhibit its activity. To achieve this, we employed molecular docking and mutagenesis studies to investigate and validate the target specificity. Additionally, we assessed the *in vivo* efficacy of the identified small molecules using a mouse bacteraemia model.

Results

SaeR is targetable for antivirulence drug development

Deletion of *SaeR* in *S. aureus* has been shown to inhibit the occurrence of skin infection, pneumonia [17], bacteraemia [18], and virus-MRSA co-infection [19]. Despite its pivotal role in pathogenesis, no SaeR inhibitors have been identified.

To demonstrate the targetability of SaeR, we used an inducible knockdown system [20]. We designed four oligos (kd-*saeR*-1–4, Supplementary Table 3) for SaeR and transformed knockdown plasmids into USA300. The knockdown effect on SaeR was determined by measuring the production of the downstream gene, *hla*. By adding 100 ng/mL of the inducer anhydrotetracycline (aTc), we found that the production of α -toxin reduced significantly (Figure 1(A)). This showed that the knockdown strain was successfully constructed. The strain harbouring pSD1-kd-*saeR*-2 (USA300-pSD1-*saeR*) was selected for further studies.

Using a skin subcutaneous infection mouse model, the pathogenicity of different deletion mutants of the *saeRS* system was assessed. Deletion of *saeR*, *saeS*, *saeQRS*, and *agrA* significantly decreased abscess size and bacterial load (Figure 1(B, C)), but deletion of *sigB* increased abscess size. In addition, complementation of *saeR* resulted in abscess sizes that were comparable to those of a wildtype strain harbouring a blank plasmid under the induction of aTc, indicating that *in vivo* induction by aTc was effective.

Although these deletion (knock-out) strains showed substantial reduction in bacterial load, they do not mimic the real-life antivirulence effect. Antivirulence molecules cannot delete or alter the genes, but they interact directly with the proteins involved in pathogenesis. Hence, a knock-down approach is more suitable to mimic the antivirulence effect. In the knockdown system, the addition of an inducer such as anhydrous tetracycline suppresses the expression of *saeR* mimicking the antivirulence effect. Using this approach, we tested whether the *saeR* can be suppressed *in vivo*.

CFU analysis revealed that the *saeR* knockdown strain reduced the size of the abscess and decreased the bacterial burden significantly (Figure 1 (D, E)). These results showed that, by inhibiting SaeR using the knock-down approach, *S. aureus* pathogenesis can be quenched *in vivo*, and SaeR is targetable for the development of antivirulence drugs.

Identification of HR3744 as an inhibitor of SaeR

After screening against 400 compounds with effects on *hla* expression, 139 compounds exhibited a repression effect on *saeP1* promoters (Supplementary Figure 1).

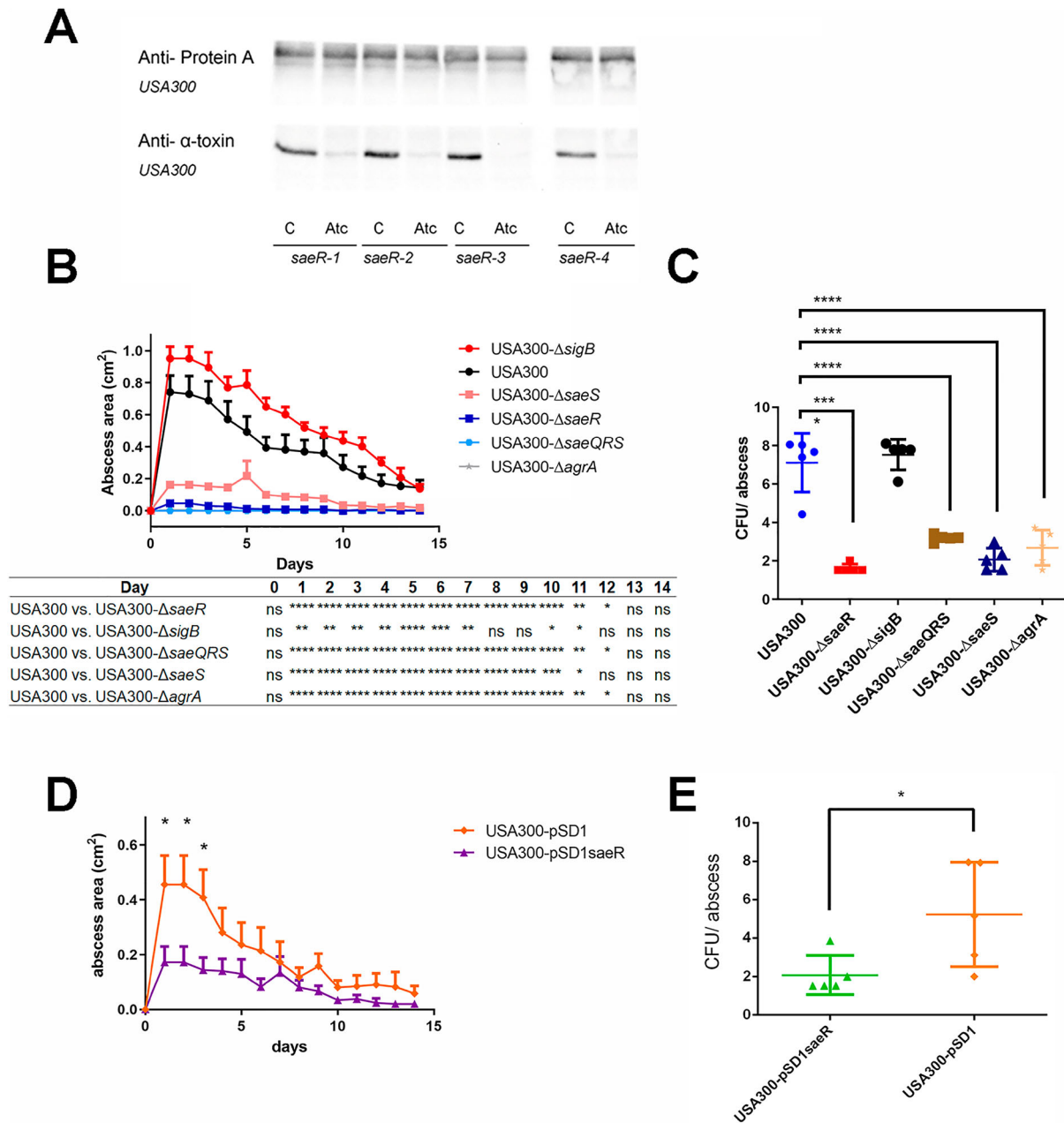


Figure 1. Targetability of SaeR by the *in vivo* knockdown approach. (A) Protein A and α -toxin production in different *saeR* knock-down strains with or without inducer aTc (100 ng/mL). (B) Abscess size (cm²) in Balb/c mice ($n=5$ /group) up to 14 days after subcutaneous (s.c.) skin injection with 50 μ L of *S. aureus* USA300 parental strain or USA300 Δ *sigB*, USA300 Δ *saeR*, USA300 Δ *saeS*, USA300 Δ *saeQRS*, and USA300 Δ *agrA*, mutant strains (5×10^7 colony-forming units [CFU]/site). (C) Bacterial load from abscesses on day 14 from mice infected with USA300 wildtype and mutant strains. (D) The mice were infected with different strains and treated with aTc orally 6 h post-infection, and the abscess size was measured up to 14 days. (E) Bacterial load on day 14 from abscesses recovered from aTc treated groups. The statistical significance was calculated by one-way ANOVA and two-way ANOVA. Data on graphs represents mean values \pm SD (* $p < .05$; ** $p < .01$; *** $p < .001$; **** $p < .0001$).

After the purification of SaeR and SaeS, a phosphorylation assay was performed (Supplementary Figure 2 (A to E)). Based on the optimized concentration of P-SaeR (Supplementary Figure 2(F)), a mixture of 10 μ M of P-SaeR and the *sae* P1 promoter were pre-treated with DMSO or 250 μ M of the compounds. After the interaction, the bound protein and DNA were examined by EMSA (Supplementary Figure 2 (G)). Compounds No. 2 and No. 3, inhibited the interaction. Therefore, after screening, HR3744 was identified as an SaeR inhibitor (Figure 2(A)). The

differential scanning fluorimetry (DSF) assay revealed that with the increasing concentration of compound HR3744, the thermal stability of SaeR decreased. This indicated that an interaction may exist between HR3744 and SaeR protein (Figure 2(B)).

Western blot analysis revealed that the compound HR3744 decreased the production of virulence factors α -toxin and Panton-Valentine Leukocidin (PVL) at various doses, but not protein A (Figure 2(C)). A dose-dependent inhibition of HR3744 against these virulence factors was observed with a concentration

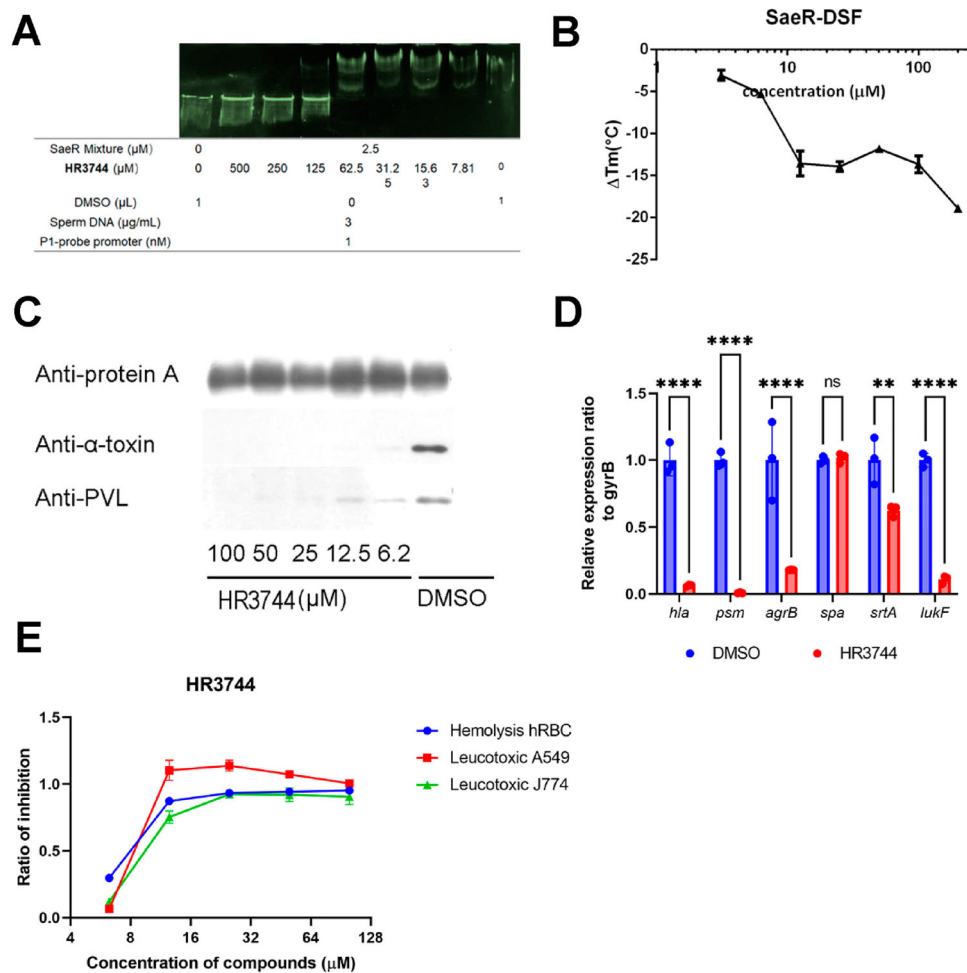


Figure 2. SaeR inhibition and antivirulence effect of HR3744 *in vitro*. (A) EMSA of SaeR bond to saeP1 promoter was inhibited by HR3744. (B) DSF analysis of HR3744 on SaeR thermal stability. Different concentrations of HR3744 (200 μM to 3.2 μM) and 5 μM SaeR were applied in this assay. (C) A dose-dependent effect of HR3744 reduced major virulence factors production. HR3744 reduced the production of two important virulence factors, α -toxin and PVL, but had no effect on protein A at different concentrations. Data collected on 5 h of culture. (D) HR3744 suppressed major virulence gene expressions by qPCR. HR3744 reduced the expression of four important virulence factors and regulators, *hla*, *psm*, *pvl*, and *agr* at a concentration of 5 μM . Data were collected on 5 h of culture. (E) Haemolysis activity against human RBC and leucotoxic activity against A549 cell and J774 cells.

ranging from 100 μM to 6.2 μM . Based on the Western blot results, the IC₅₀ for the production of α -toxin and PVL was less than 6.2 μM . The overall impact on the virulence genes expression was further assessed using Quantitative Polymerase Chain Reaction (qPCR). Similar to the Western blot results, HR3744 reduced the expression of *hla*, *pvl*, and other virulence genes such as *psm* and *agr* (Figure 2(D)). In addition to the Western blot and qPCR, haemolysis and leucotoxicity assays were carried out using HR3744. The novel small molecule demonstrated dose-dependent reduction of staphylococcal haemolysis activity against human RBC and leucotoxicity against macrophage J774 cells, and epithelial A549 cells respectively (Figure 2(E)).

The cytotoxic effect of HR3744 was tested using Raw264.7 cells. The TC₅₀ of HR3744 in this cell line was found to be greater than 200 μM , suggesting that the drug does not induce any cytotoxic effect at lower concentrations. In addition, HR3744's MIC against *S. aureus* USA300 was more than 240 $\mu\text{g/mL}$

(500 μM). Thus, results from these findings exemplifies the importance of non-toxic, and non-antibiotic antivirulence molecules such as HR3744, which suppress *S. aureus* pathogenesis by inhibiting the expression of virulence factors without any killing effect. These preliminary *in vitro* findings directed us to explore the target specificity of HR3744.

Target specificity of HR3744

The target specificity of HR3744 against SaeR was determined by analysing the expression of *hla* in wild-type and mutant strains. In the wildtype USA300 strain, HR3744 inhibited the fluorescence signal with an EC₅₀ of approximately 10 μM , but the EC₅₀ in the *saeS* and *saeR* deletion strains were greater than 100 μM . Additionally, we found that the EC₅₀ of HR3744 in the *agrA* deletion strain was approximately 25 μM , demonstrating that HR3744 does not suppress *hla* production by inhibiting AgrA, but rather SaeR (Figure 3(A)).

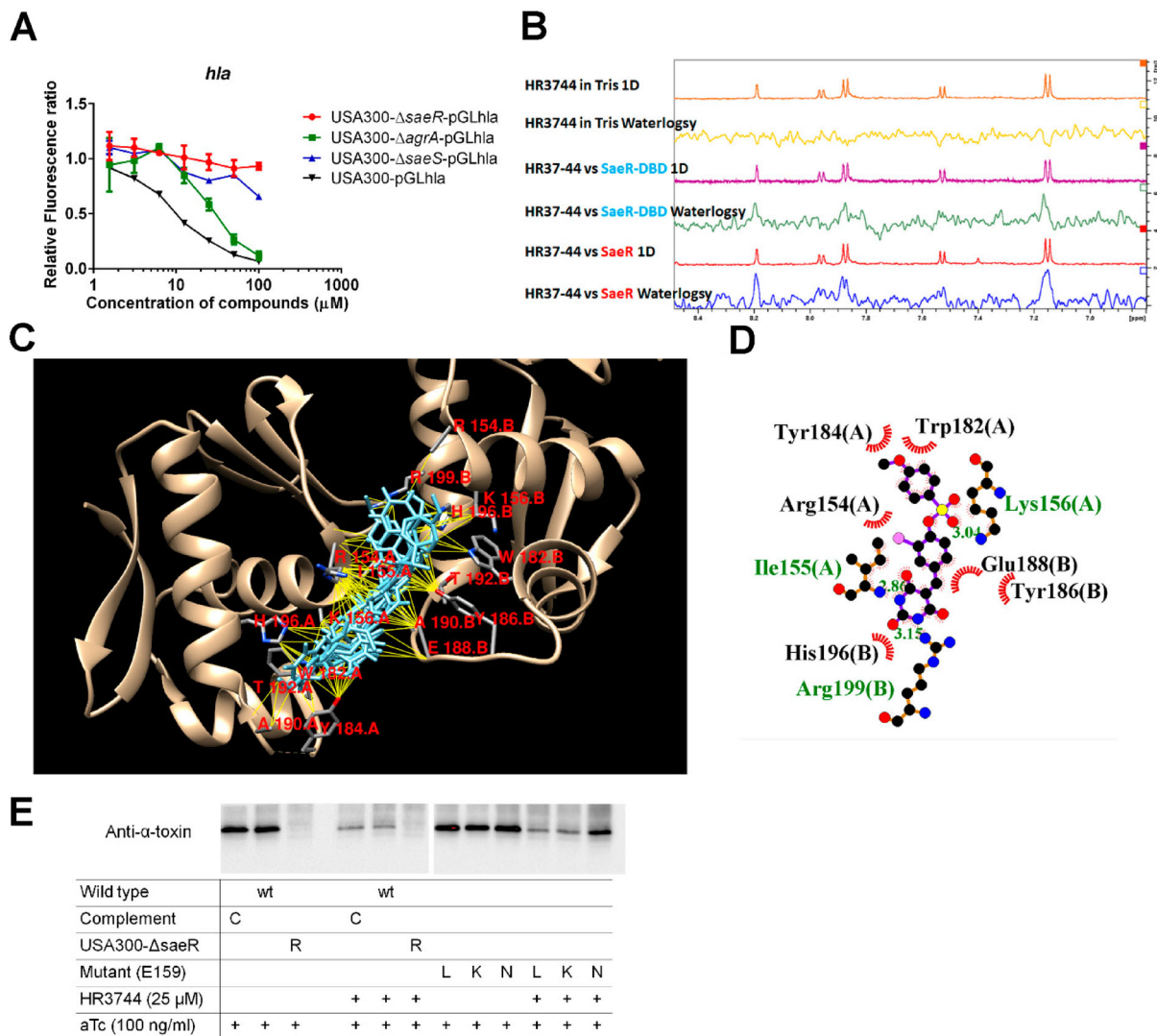


Figure 3. Target specificity of HR3744 against SaeR. (A) The EC₅₀ of HR3744 against *hla* expression by testing fluorescence signal in different mutant strains, USA300, USA300-ΔsaeR, USA300-ΔagrA, and USA300-ΔsaeS. (D) WaterLOGSY of 0.8 μM SaeR or SaeRDBD with 40 μM HR3744. (C) Predicted binding conformations of HR3744 to SaeR. The SaeR of *S. aureus* (PDB entry 4ixa) is labelled in cyan. HR3744 is predicted to bind near the binding cavity of SaeR to DNA. The side chains of the predicted interacting amino acid residues that participate in the hydrophobic contacts with HR3744 are shown. (D) A 2D schematic diagram of SaeR-HR3744 interactions is shown. Hydrophobic contacts are represented by an arc with spokes radiating towards the HR3744 atoms that they contact. The contacted atoms in HR3744 are shown with spokes radiating back. (E) α-toxin production in different strains with or without HR3744. Example of the response of site-mutagenesis of amino acid E159 to the inhibition activity of HR3744.

EMSA was used to assess the inhibition of HR3744 against SaeR, while NMR water ligand-observed gradient spectroscopy (waterLOGSY) was used to confirm direct interaction of SaeR and HR3744. In 1D spectroscopy, the compound HR3744 exhibited some typical peaks; however, no positive peaks were identified during waterLOGSY detection. When SaeRDBD or SaeR was introduced to the system, positive characteristic peaks were detected in waterLOGSY spectroscopy. These results demonstrated the direct interaction between HR3744 and SaeR or SaeRDBD (Figure 3(B)).

Virtual docking and mutagenesis

The virtual docking method was applied to investigate the interaction of HR3744 with the relative amino

acids of the SaeR protein. Computer-simulated docking utilizing a grid box that encompasses the full crystal structure of SaeR (PDB:4qwq and 4ixa) indicated that HR3744 might fit into the pocket between the two monomers (Figure 3(C) and Supplementary Figure 3(A)). To limit the likelihood of missing a potential interaction, we retained all seven conformations of HR3744, with yellow lines representing the interactions between HR3744 and SaeRDBD (Figure 3(C)). To clearly analyse the interaction between SaeR and HR3744 by ligplus in one conformation (Figure 3(D)), direct hydrophobic interactions with residues R154, R155, K156, W182, Y184, Y186, E188, H196, and R199 were indicated. Other conformations were presented in Supplementary Figure 3 (B to G). In summary, direct hydrophobic contacts with residues M153, R154, R155, K156, W182, Y184,

Table 1. Mutagenesis of SaeR.

| Mutant | Amino acids | Activity | HR3744 inhibition |
|----------|-------------|----------|-------------------|
| Wildtype | | +++ | C |
| 1 | P152A | +++ | C |
| 2 | M153A | – | |
| 3 | R154L | – | |
| 4 | R154E | – | |
| 5 | R154N | +++ | C |
| 6 | I155G | +++ | C |
| 7 | K156L | – | |
| 8 | K156E | – | |
| 9 | K156N | – | |
| 10 | E159L | + | C |
| 11 | E159K | ++ | C |
| 12 | E159N | ++ | R |
| 13 | W182L | – | |
| 14 | Y184A | – | |
| 15 | D185L | ++ | C |
| 16 | D185H | ++ | C |
| 17 | D185N | ++ | R |
| 18 | Y186A | – | |
| 19 | E188L | ++++ | S |
| 20 | E188K | – | |
| 21 | E188N | ++ | S |
| 22 | D189L | – | |
| 23 | D189H | +++ | S |
| 24 | D189N | – | |
| 25 | A190G | ++ | C |
| 26 | N191L | – | |
| 27 | T192A | – | |
| 28 | H196L | + | C |
| 29 | H198L | + | C |
| 30 | H198D | – | |
| 31 | R199L | – | |

+: mutant showed activity on production of α -toxin; –: no production of α -toxin; the more "+," the higher the activity of SaeR. C: Similar inhibition as a control; S: mutants became sensitive to HR3744; R: mutants became resistant to HR3744.

Y186, E188, A190, T192, H196, and R199 were identified in the conformations (Figure 3(C) and Supplementary Table 1).

Based on the probable binding sites identified through our docking models, we made site-directed modifications along the expected binding pocket by substituting the original amino acid residues with a short side chain or by altering the polarity (Table 1).

By transforming mutation plasmids into USA300- Δ saeR, we explored whether the deletion of *saeR* may be compensated by other *saeR* mutants through the synthesis of α -toxin. Interestingly, 16 of the 31 mutants did not produce α -toxin despite aTc induction (Table 1). Our results also suggested that these amino acids are essential for the function of SaeR. Ten mutant strains did not alter the susceptibility to HR3744. However, strains with SaeR mutation at E188L, E188N, and D189H became sensitive to HR3744, whereas, E159N and D185N showed resistance to HR3744.

In the wildtype SaeR complementation strain, HR3744 exhibited the similar suppression of α -toxin production as that for the wildtype strain. However, the *saeR* deletion strain did not produce α -toxin, irrespective of the presence of HR3744. It is noteworthy to mention that two mutant strains with amino acids replacement in SaeR from glutamic acid at position 159 to leucine and lysine exhibited the suppression

of α -toxin production in the presence of HR3744. Their level of suppression was similar to the complementation strain. But in another strain with a mutation in position 159 to asparagine (E159N) displayed resistance to HR3744 (Figure 3(E)). These findings suggested that HR3744 might target SaeR via interacting with the amino acid glutamic acid at position 159 (E159).

Structure–activity relationship (SAR)

To further understand the property of HR3744, we conducted SAR studies. Through this approach, we aimed to discover analogues of HR3744 with increased SaeR inhibition properties. We searched the analogues of HR3744 in the Hits2lead database and found 79 compounds available with 85% similarity. Using luminescence and fluorescence signals in USA300-pGLhla, the antivirulence effect of the newly identified analogues against *hla* expression was investigated. To exclude the possibility of a substance altering the luminescence or fluorescence reading, we constructed a novel system in which the kanamycin resistance gene was placed downstream of the *hla* promoter. The USA300-pGLhla (Supplementary Figure 4 (A)) developed resistance to kanamycin in the absence of an SaeR inhibitor; however, the addition of HR3744 was found to re-sensitize the bacterium to kanamycin (Supplementary Figure 4(B)). Using this method, we analysed the analogues of HR3744. Finally, we selected those compounds which showed inhibition in all the *in vitro* assays (Supplementary Figure 4 (C and D)). Using these results, structure activity relationship was established for the analogues.

Based on the inhibition results of the tested benzylidene barbituric acid and benzylidene thiobarbituric acid derivatives, the SAR paradigm is summarized in Figure 4(A). The substituents on the two nitrogen atoms in the (thio)barbituric acid segment (R¹ and R²) and the *meta/para*-positions on the benzylidene segment (R⁴ to R⁶) were found to be important for the activity, while keeping *ortho*-substituents R³ and R⁷ as H/H were beneficial. In general, for R¹ and R², both H/H and H/Me combinations were favoured, while substitution with two Me groups or one or two bulky groups like phenyl gave lower activity. For R⁴ and R⁶, the combinations, such as Cl/Cl, EtO/Br, EtO/H, and Br/H were favoured, while H/H and bulky groups like aromatic sulphonates were disfavoured. For R⁵, the substituents comprising a hydrophobic aromatic ring and an O-containing flexible spacer (e.g. benzyloxy group and aromatic sulphonates) were favoured. In contrast, the linear flexible groups without an aromatic ring gave lower activity. Finally, both barbituric acid and thiobarbituric acid contributed similarly to the activity. Considering the stability issue caused by the base labile sulphonate

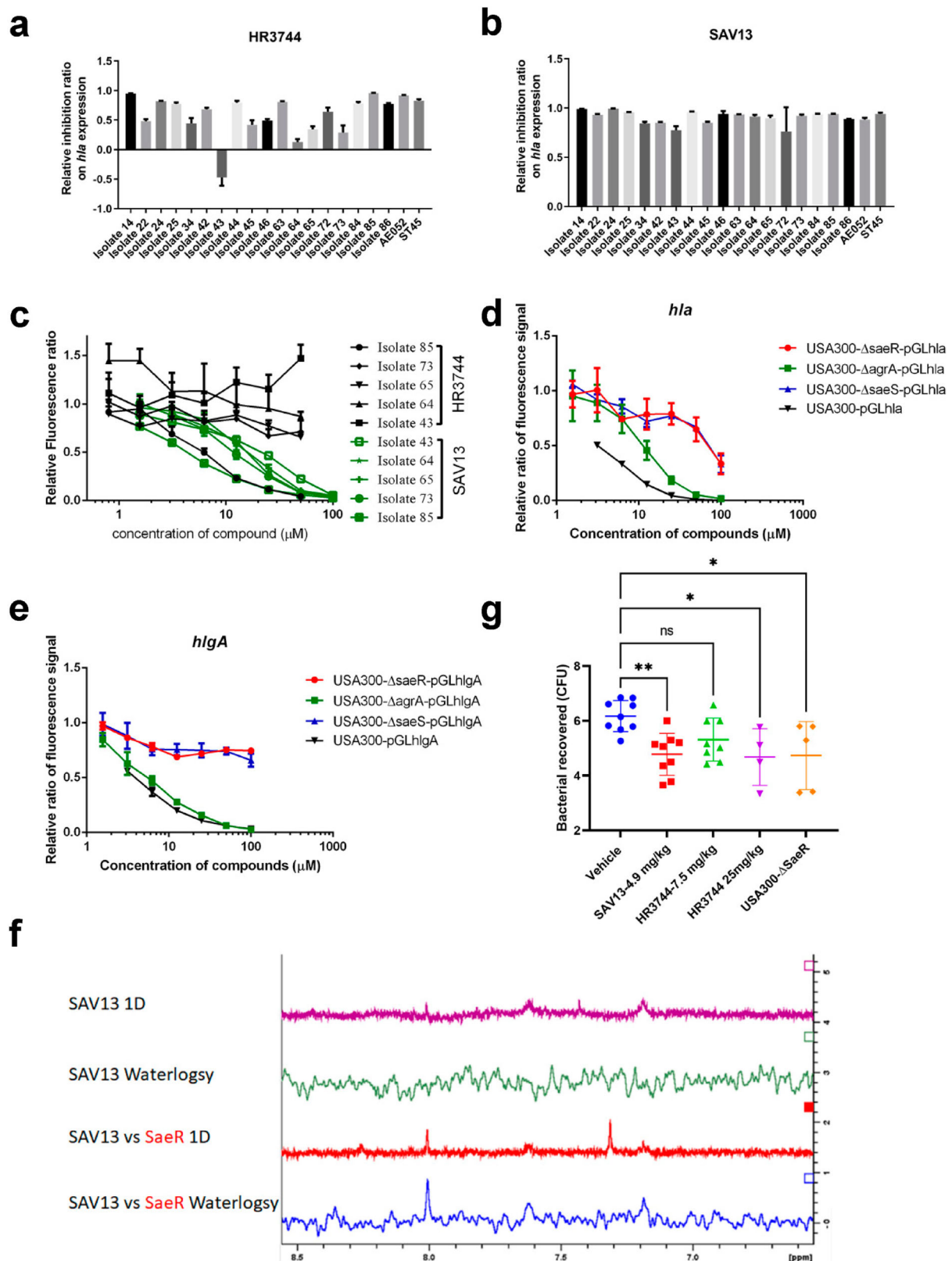


Figure 5. Antivirulence effect comparison of HR3744 and SAV13 *in vitro* and *in vivo*. (A) The inhibition of HR3744 at 50 μM on *hla* expression in 20 clinical isolates harbouring pGLhla plasmid was evaluated by detecting fluorescence signal. (B) The inhibition of SAV13 at 50 μM on *hla* expression in 20 clinical isolates harbouring pGLhla plasmid was accessed by detecting fluorescence signal. (C) Selected isolates showed different responses to HR3744 and SAV13 and isolate 85 showed a similar response against two compounds as a control. (D) The EC50 of SAV13 against *hla* expression by testing fluorescence signal in different mutant strains, USA300, USA300- ΔsaeR , USA300- ΔagrA , and USA300- ΔsaeS . (E) The EC50 of SAV13 against *hlgA* expression by testing fluorescence signal in different mutant strains, USA300, USA300- ΔsaeR , USA300- ΔagrA , and USA300- ΔsaeS . (F) WaterLOGSY of 0.8 μM SaeR with 40 μM SAV13. (G) Bacterial load of *S. aureus* USA300 or USA300- ΔsaeR in the kidney of mice after i.v. infection in the presence or absence of HR3744 and SAV13 treatment at different dosages. The statistical difference was calculated by one-way ANOVA. All data represent mean values \pm SD ($*p < .05$; $**p < .01$).

all 20 clinical isolates at a dose of 50 μM with a ratio of inhibition that varied among isolates (Figure 5(B)). The HR3744-resistant isolates, No. 43, 64, 65, and 73, become sensitive to SAV13 (Figure 5(C)). By q-PCR analysis, we analysed some other genes modulated by SaeR. Deletion of SaeR showed reduced expression of *chp*, *hlgA*, *hlgC*, *map*, and *splA*, while enhanced the expression of *ureA* (Supplementary Figure 5). The inhibitors, HR3744 and SAV13 showed a similar effect as *saeR* deletion strain on decreasing the expression of *chp*, *hlgA*, *hlgC*, *map*, and *splA*, however, increased *ureA* expression even stronger than deletion of SaeR.

By measuring the fluorescence signal of pGLhla in USA300 including various regulator deletion mutants, the target specificity of SAV13 was further examined. SAV13 inhibited *hla* expression in the USA300 strain with EC50 around 3, and 10 μM in the *agrA* deletion mutant, while around 80 μM in *saeR* or *saeS* deletion strains (Figure 5(D)). Similar results were found for *hlgA* expression and EC50 values for SAV13 against USA300-pGLhlgA and USA300- Δ *agrA*-pGLhlgA, which were approximately 3 and 5 μM , respectively. Whereas, for USA300- Δ *saeR* and USA300- Δ *saeS*, the EC50 values were greater than 100 μM (Figure 5(E)). By detecting the physical binding of SAV13 to SaeR, the positive peaks from the waterLOGSY panel were observed, indicating the interaction between SaeR and SAV13 (Figure 5(F)).

After analysing the *in vitro* activities of HR3744 and SAV13, we investigated their *in vivo* effectiveness in several animal models. To evaluate the efficacy of SaeR inhibitors, a mouse bacteraemia model was used. Mice were infected with the *saeR* deletion mutant or *S. aureus* USA300 wild-type strains and treated with high dose of HR3744 or low dose of SAV13. CFU analysis revealed similar amount of bacteria from their kidneys in treatment groups was recovered (Figure 5(G)). Significant differences in the bacterial load were observed between mutant, treatment, and control groups ($p = .0075$ for wildtype and *saeR* deletion mutant, .0011 for vehicle and SAV13 at 4.9 mg/kg, .0413 for vehicle and HR3744 at 7.5 mg/kg, and .066 for vehicle and HR3744 at 25 mg/kg).

Discussion

S. aureus has acquired resistance to practically all known antibiotics, necessitating the discovery of new therapeutic targets and the development of novel strategies to treat infections caused by this pathogen [5,21,22]. Surface-associated virulence factors, exotoxins, enterotoxins, and superantigens contribute to the pathogenicity of *S. aureus* [23]. Exotoxins from *S. aureus*, including α -toxin, β -toxin, δ -toxin, PVL, and Phenol-Soluble Modulins (PSMs), all contribute

to the lysis of leukocytes [24], and α -toxin and PSMs may also contribute to the formation of biofilms [25,26]. Protein A, fibronectin-binding protein A/B, and envelope-associated proteins are essential for the adherence and penetration of *S. aureus* in epithelial cells and for the development of abscesses in host tissues [27]. Although upstream regulators control multiple virulence factors, suppression of these regulators may not completely eliminate the expression of virulence factors. Sometimes, the inhibition of upstream regulator may enhance the expression of some virulence factors [27]. Hence, by targeting downstream regulator (wherein the majority of virulence factors are under strict control), we can effectively suppress the expression of virulence factors. Thus, these regulators may offer effective and promising therapeutic potential.

SaeR as a downstream regulator in the *saeRS* two-component system can modulate many downstream genes such as surface proteins (Spa, FnbA, Emp), secreted proteins (SspA, HlgA, CHIPS, SplA), purine synthesis pathway, pyrimidine biosynthetic pathway, and arginine deiminase pathway, etc. Up-regulating genes include lactose metabolic pathway genes (*lacA-G*), urea catabolytic enzymes urease (*ureA-G*) [28]. Since *saeR*-regulated genes are essential for *S. aureus* pathogenesis, by targeting this protein, we can develop novel anti-infective agents against *S. aureus*. With this unique approach, our present study provided an evidence for developing anti-virulence agents against MRSA.

Previous studies employing *saeR* deletion strains showed reduced *S. aureus* pathogenesis in various infection models [29–31]. Despite these findings, the application of *saeR* deletion strains for antivirulence *in vivo* studies has some limitations. Firstly, *saeR* is pivotal for infection initialization. When we use *saeR* deletion mutant, *S. aureus* fails to cause infection in mice. Hence, *saeR* deletion strain may not help us determine whether the antivirulence drug is effective in reducing *S. aureus* pathogenesis. Also, due to the non-antibiotic property of antivirulence molecules, comparing the bacterial load between the wild-type, compound-treated, and *saeR* deletion groups is not ideal to determine whether *saeR* is a druggable target for the development of antivirulence therapy. Secondly, *saeR* deletion blocks the spread of a bacterial infection. But it may have little impact on reducing the symptoms at the site of infection. Hence using deletion mutant, we cannot compare whether the antivirulence drug-treated group reduced the symptoms at the site of infection. To address these lacunae, we constructed CRISPR-dCas9-based knockdown plasmid and validated that SaeR is a targetable protein for antivirulence drug development under *in vivo* conditions. The *in vivo* knockdown of *saeR* simulated the antivirulence therapy for *S. aureus* infection, wherein

we first established the infection and then began the treatment using an inducer aTc. When compared to the mice group infected with a strain harbouring blank plasmid, aTc treated group showed substantial reduction in bacterial load and abscess size. These findings validated the suppression of *saeR* expression by aTc and proved that this protein is targetable.

To investigate antivirulence activity, an *hla*-kan system was developed. Unlike the earlier approach that monitored virulence gene expression using luminescence and fluorescence signals [32], the *hla*-kan system utilized bacterial survival in media containing kanamycin. Our earlier studies using *gfp*-lux dual reporter system revealed many false-positive results [33]. Thus, an improved screening approach based on the growth of bacteria in the presence of kanamycin was developed. This novel *hla*-kan screening approach was found to be more efficient and served as a supplement for the dual-reporter-based screening system. The *hla*-kan system is regulated by the *hla* promoter and *S. aureus* can grow in kanamycin treated growth media only when the *hla* is actively expressed. When compounds suppress the activity of *hla* promoter, the bacteria cannot grow in presence of kanamycin (Supplementary Figure 4(B)). Thus, by combining the dual reporter system with the *hla*-kan system, we significantly reduced false-positive candidates. Additionally, while creating this *hla*-kan system, many antibiotic-resistant genes such as kanamycin/neomycin (kan/neo), erythromycin (*ermC*), beta-lactamase (NDM-1), and rifampicin (*rif*) were assessed for compatibility. Only kan/neo demonstrated a dose-dependent response to the presence of the repressor. By using this approach, SAR analysis was performed. An analogue of HR3744 called SAV13 was identified through SAR, which showed *hla* suppression effect in both *hla*-kan and dual-reporter systems.

According to qPCR results, secreted virulence factors such as α -toxin, PVL, and PSMs were repressed by HR3744. This finding suggested that HR3744 reduced renal infection by suppressing the expression of these key virulence factors. Since protein A (*spa*) is not regulated by SaeR [12], no differences were observed between the bacteria treated with DMSO or HR3744. However, HR3744 and SAV13 both down-regulated the expression of HlgA and HlgC, and suggested that the SaeR inhibitors reduced bacterial survivability in blood stream by repressing γ -haemolysin production [34]. Chemotaxis inhibitory protein of *S. aureus* (CHIPS, encoded by *chp*) is an exoprotein and a potent inhibitor of neutrophil and monocyte-mediated chemotaxis. This virulence factor protects *S. aureus* from host innate immune response and increases its survivability [35]. The suppression of CHIPS by HR3744 and SAV13 may make the bacteria susceptible to innate immune response and thus lead to the decrease in bacterial load during bacteraemia

infection. The Map (MHC class II analogue protein) protein, is a secreted protein that can bind to a variety of extracellular membrane components, including fibronectin, fibrinogen, vi-tronectin, bone sialoprotein, and thrombospondin [23]. A decrease in Map expression could inhibit bacterial attachment to host tissue during infection. *S. aureus* secretes 6 serine protease-like proteins (SplA-SplF). These Spls are involved in a variety of chronic ailments, such as asthma and pneumonia, resulting in disseminated lung injury. By cleaving the glycosylated cell surface protein mucin 16, SplA reportedly promotes bacterial invasion and dissemination in lung tissues [36]. Therefore, inhibition of SaeR may prevent chronic infection and bacterial invasion. In addition to suppressing certain virulence genes, HR3744 and SAV13 increased the expression of *ureA*. Urease is an essential component of the acid response in *S. aureus*. It is an essential enzyme required for persistent kidney infections and subsequent staphylococcal metastasis. Studies have shown that CcpA and Agr upregulate urease gene transcription, whereas CodY and SaeR downregulate its expression [28,37]. Thus the increased expression of *ureA* gene in the presence of HR3744 and SAV13, suggested that the inhibitors may modulate the expression of *ureA* through inhibiting SaeR.

The specificity of the target was determined using three methods: chemical genetics; genetics; and mutagenesis [33]. Using a chemical genetics technique, we discovered that an analogue of HR3744 called HR3763 with a minor modification (one bromide), lost its effectiveness against *S. aureus*. This shows that the inhibition of SaeR by HR3744 was selective and that the structure of the inhibitor was crucial for its effectiveness. We examined *hla* expression in the *saeR* deletion strain using a genetic method. Due to the deletion of HR3744's target, *S. aureus* exhibited resistance to HR3744's antivirulence action. It was also demonstrated that SaeR was the target of HR3744. By using site-directed mutagenesis, we found that a mutation at position 159 from E to N in SaeR protein had no influence on the expression of the downstream gene *hla*. A reduced susceptibility of SaeR-E159N against HR3744 was observed. Hence, this SaeR-E159N resistance suggested that HR3744 modulated *hla* expression by inhibiting SaeR. Even though the crystal structure and NMR structure of SaeR and HR3744 have not yet been reported, the data from our chemical genetics, genetics, and mutagenesis studies demonstrated target specificity.

By analysing the structure-activity relationship, we discovered that an analogue of HR3744 SAV13 exhibited a five-fold increase in antivirulence activity. These lead compounds (HR3744 and SAV13) not only demonstrated *in vitro* antivirulence efficacy, but also *in vivo* therapeutic effect. Through this study, we illustrated the application of chemical genetics to discover

novel antivirulence agents against a major downstream virulence regulator SaeR. This constitutes the initial stage in the development of an antivirulence agent, and we aim to continue developing this type of agent. In the future, this kind of medication may function as an antibiotic adjuvant or even replace antibiotics in certain circumstances.

To conclude, our research showed that SaeR is a potential druggable target for the development of antivirulence agents. *In vivo* knockdown is a suitable method for investigating the targetability of a target. The antivirulence small molecule HR3744 interacts with the amino acid E159 of SaeR protein. This specific interaction displayed SaeR inhibition which resulted in the reduced expression of *hla* and other virulence factors. Analogue of HR3744 named SAV13 may serve as the lead molecule for optimizing SaeR inhibitors. Both HR3744 and SAV13 demonstrated *in vivo* effectiveness against *S. aureus* infection in mice. By combining these compounds with antibiotics, they may function as antibiotic adjuvants with an *in vivo* synergistic effect.

Materials and methods

Materials

The bacterial strains used in this study are listed in Supplementary Table 2. Brain heart infusion (BHI) broth and BHI agar plates were used throughout for growing *S. aureus*. Chloramphenicol was used at 10 µg/mL. Unless otherwise stated, all cultures were grown aerobically at 37°C with shaking, and growth was monitored at 600 nm with a HITACHI U-2800 (Hitachi, Japan) spectrophotometer.

Hla-kan system

To generate the plasmid pGLhla-kan system, respective PCR primers (Supplementary Table 3) were used to amplify the *hla* promoters from *S. aureus* USA300 FPR3757 chromosomal DNA and kanamycin resistance gene from plasmid pKan. The amplicons were combined and another set of PCR was carried out to ligate both amplicons using forward primer of the *hla* promoter and reverse primer of *kan*. The resulting combined amplicon called *hla-kan* was restriction digested with NheI/NotI double-digestion enzymes and ligated with pGL plasmid which was digested with the same restriction enzyme(s). All of the plasmid constructs and PCR products were verified by sequencing.

Minimum inhibitory concentration (MIC) tests

Antibiotics which were serially diluted were used for MIC and were determined by inoculating 5×10^4 *S. aureus* cells in 100 µL BHI medium in 96-well plates.

The MIC was defined as the minimum concentration resulting in a cell density less than 0.01 OD at 620 nm [38,39], which corresponded to no visible growth, after incubating for 18 h at 37°C.

Construction of *S. aureus* gene deletion mutants

Plasmid pKOR1-*saeR*, pKOR1-*saeS*, pKOR1-*saeQRS* were transformed into *S. aureus* USA300. The resulting transformant was used to delete genes in *S. aureus* via a previously reported procedure [40]. Deletion of genes were further confirmed by PCR and sequencing.

Disk diffusion and lux assays

A single colony of bioluminescent *S. aureus* strains with plasmid pGLhla or pGLspa (Supplementary Table 2) from BHI agar was resuspended in 200 µL of sterile water. Later, this bacterial suspension was mixed with 75 mL of 0.7% (w/v) soft agar (375-fold dilution), and overlaid onto BHI agar plates. Antibiotic disks (Becton Dickinson, Mississauga, ON, Canada; Difco, Detroit, MI, USA) were placed on the overlay, and the plates were incubated at 37°C. After 20 h, inhibition zones were measured and luminescence was detected with Xenogen IVIS 100 *in vivo* imaging system (Xenogen, Alameda, CA).

Gene expression measurement of bacterial cultures

For quantification of GFP and bioluminescence, overnight bacterial cultures of different strains with plasmid pGLhla were diluted in an appropriate medium containing 10 µg/mL chloramphenicol. Samples (100 µL) were transferred into a microtiter plate from culture tubes, and fluorescence was measured by using a DTX 800/880 multimode plate reader (Beckman). Bacteria with pGL plasmid were included as a control to allow correction for background fluorescence. For growth curve analysis, 100 µL of 10^6 *S. aureus* strains were loaded to 96-well microtiter plates in triplicate and incubated at 37°C. The optical density at 620 nm (OD_{620}), the fluorescence (GFP, Ex/Em: 485/535), and the bioluminescence were measured every 30 min in the DTX 800/880 multimode plate reader (Beckman).

Screening to identify *saeR* inhibitors

A platform with a total of 20 *gfp-luxABCDE* dual-reporter plasmids with selected promoters from *S. aureus* virulence-associated genes was constructed [32]. The screening against *hla* promoter activity from USA300-pGLhla was conducted with 50,240 compounds. A total of 670 compounds were found

to repress 65% activity of *hla* promoter. Out of 670 hit compounds, 400 showed reproducible repressive effects on *hla* promoter activity [33]. Screening against the promoter saeP1, was conducted to test luminescence, OD600, and fluorescence as mentioned above.

Differential scanning fluorimetry (DSF)

The DSF was conducted as previously described [41]. The fluorescent dye SYPRO orange (Sigma–Aldrich), an environmentally sensitive fluorophore, was used to monitor the unfolding of SaeR. This assay was performed using the Vii 7 Real Time PCR Detection System (Bio-Rad).

Samples for this assay were prepared by adding 50 µL each of SaeR (final concentration, 2 µM), 5X SYPRO orange, serial dilution of HR3744 (DMSO < 1%), and DSF buffer (150-mM NaCl and 10-mM HEPES [pH 7.5]) to the 96-well, 0.2-mL optical PCR plate in triplicate. The plate was heated from 25°C to 90°C at a rate of 1°C/min. The fluorescence intensity was measured with Ex/Em: 490 nm/530 nm. The data was processed as previously described [41].

Western blot

Bacterial culture of *S. aureus* strains treated with compounds and grown under shaking condition for 24 h were collected. After adjusting the OD600 with BHI broth, supernatants were extracted after centrifuging the bacteria at high speed. The extracted supernatant was boiled in Laemmli sample buffer and 5 µL of this suspension were loaded into 12% sodium dodecyl sulfate-polyacrylamide gel. Alpha-toxin was detected using rabbit anti-staphylococcal α-haemolysin antibody (1:20,000) (Sigma–Aldrich) and goat horseradish peroxidase (HRP)-conjugated anti-rabbit IgG (1:5000) (Sigma–Aldrich). Protein A was visualized using HRP-conjugated rabbit anti-staphylococcal Spa antibody (1:20,000) (Abcam). PVL was identified using Rabbit anti-staphylococcal Leukocidin F (LukF) antibody (1:20,000) (IBT). The Western blot protocol was performed as described in the product guide for Amersham ECL Western blotting detection reagents (GE Healthcare, Buckinghamshire, United Kingdom).

Isolating human erythrocytes (HRBC)

Whole blood was centrifuged at 500×g for 10 min at 4°C, and supernatant (plasma) was aspirated. Erythrocyte pellet was resuspended with double volume of HBSS. Another centrifugation at 500×g for 10 min at 4°C was conducted and the supernatant was discarded. This step was repeated three times or until the disappearance of colour in the supernatant. Erythrocyte was diluted to respective concentration, and stored at 4°C.

Haemolysis assay on HRBC

Total haemolysis assay was conducted as described previously [33] using human erythrocytes. Briefly, 50 µL of human erythrocytes (5×10^6 /mL) were added to microtiter plates (Cellstar TC; Greiner, Germany), which were pre-filled with 50 µL of serial dilutions of bacterial culture supernatants, and incubated for 60 min at 37°C. As a positive control, ddH₂O was used in each assay, whereas, phosphate-buffered saline served as a negative control. Following centrifugation, the absorption at 450 nm (A450) of the resultant supernatants was determined with a Multimode detection DTX plate reader (Beckman, Germany). All experiments were performed in triplicates and three independent assays were carried out.

Leucotoxic assay

J774.1 mouse macrophage cells (ATCC TIB-67) were cultured in DMEM medium supplemented with 10% fetal bovine serum (Invitrogen). A549 mammalian lung epithelial cells were grown using MEM medium supplemented with 10% fetal bovine serum. Cells were seeded in 96-well plates at a density of 5.0×10^4 cells per well. Later, 10 µL of staphylococcal suspension was added to 90 µL of cell culture medium per well. Following incubation at 37°C for 6 h, cell viability was measured using 3-(4,5-dimethylthiazol-2-yl)-2,5-diphenyltetrazolium bromide (MTT) assay. Ten microliters of a freshly prepared solution of MTT (5 mg/mL; Sigma, Paris, France) in sterile PBS was added to each well. The plates were incubated at 37°C in 5% CO₂ for 4 h. Then, 100 µL of lysis buffer (10% SDS, 0.1% hydrochloric acid) was added to each well. After an overnight incubation at 37°C, the optical densities at 540 nm were measured with a DTX880/800 plate reader [42,43].

Protein expression and purification

The plasmid for expressing full-length SaeR and cytosol part of SaeS (SaeS^C) were obtained from Prof. Taek Bae and Prof. Victor J Torres, respectively. The SaeRDBD amplicon was amplified by PCR from USA300 genomic DNA, and then cloned into pET28a plasmid. After transforming the plasmids in *E. coli* Bl21 (DE3) strain, proteins were overexpressed by growing the respective strains in LB broth at 20°C and induction with 0.5 mM isopropyl β-D-1-thiogalactopyranoside (IPTG). Three-tier purification process was followed for isolating SaeR, SaeRDBD, and SaeS^C. First we started with metal affinity (Hitrap His-tag column), followed by anion exchange (MonoQ, GE Healthcare), and then size-exclusion chromatography (Superdex 200, GE Healthcare) was

employed to isolate the purest form of SaeR, SaeRDBD, and SaeS^C proteins. Additionally, full-length *saeS* amplicon was cloned into pRhisMBP plasmid. After successful transformation and overexpression in *E. coli* Bl21 (DE3) strain, purification was performed using a His-trap column and a maltose binding protein (MBP) column. The MBP tag was finally removed by tobacco etch virus protease on the TEV site between the MBP and the target protein.

Phosphorylation assays

The kinase assays were performed in the presence of 20 μ M SaeR and 1 μ M SaeS^C in kinase buffer (10 mM Tris-HCl, pH 7.4, 50 mM KCl, 5 mM MgCl₂, 10% glycerol). The final reaction mixture volume was 20 μ L. To initiate the kinase reaction, 2 μ L of ATP (100 μ M) was added. The reaction mixtures were kept at RT for 30 min, and then the ADP released by the reaction was measured with the ADP-Glo Kinase Assay kit (V9101, Promega, Madison, WI, USA).

Electrophoretic mobility shift assay (EMSA)

Purified SaeR (20 μ M) and SaeS^C (1 μ M) were mixed together in phosphorylation buffer (10 mM Tris-HCl, pH 7.4, 50 mM KCl, 5 mM MgCl₂, 10% glycerol). One mM ATP was then added, and the mixture was incubated at RT for 5 min. Later, FAM-labelled DNA probe was added to the mixture. The phosphorylation was confirmed by phosphorylation assay. For electrophoretic mobility shift assay (EMSA), the entire reaction mixture was used. DNA probes were PCR amplified with FAM-labelled primers and the labelled probe (80 ng) was mixed with various amounts of the test protein in 25 μ L of gel shift loading buffer (10 mM Tris-HCl, pH 7.4, 50 mM KCl, 5 mM MgCl₂, 10% glycerol, 3 μ g/mL sheared salmon sperm DNA). After incubation at RT for 30 min, the samples were analysed by 8% PAGE (100 V for pre-run, 85 V for 85 min for sample separation). The gels were then imaged with a Typhoon scanner (genome centre, HKU).

Cytotoxicity assay

The cytotoxicity of compounds in different cell lines, J774.1, Raw264.7, Vero, and Hep2 cells were evaluated by MTT assay according to the manufacturer's instructions and performed according to our previous study [33]. In brief, ten microliters of a freshly prepared solution of MTT (5 mg/mL; Sigma, Paris, France) in sterile PBS was added to each well. The plates were incubated at 37°C in 5% CO₂ for 4 h. Then, 100 μ L of lysis buffer (10% SDS, 0.1% hydrochloric acid) was added to each well. After an overnight incubation at 37°C, the optical densities at 540 nm were measured with a DTX880/800 plate

reader. The highest concentration of compound used was 500 μ M. GraphPad Prism (version 8.0) was used for graph plotting. Experiments were carried out in triplicate and repeated twice for confirmation.

Water ligand-observed gradient spectroscopy (WaterLOGSY)

WaterLOGSY, a ligand-observed NMR technique, was used to screen for HR3744 or SAV13-interaction with SaeR [44]. WaterLOGSY experiments were conducted on a 600-MHz Bruker Avance spectrometer using a 5-mm PASEI probe. The pulse scheme used for the WaterLOGSY experiment was “ephogsygpno.2” with water suppression using excitation sculpting with gradients. All experiments were conducted at 298 K using 5-mm-diameter NMR tubes with a sample volume of 500 μ L and 40 μ M HR3744 or SAV13 supplemented and recorded using 4 K scans. All samples were dissolved in 95% H₂O and 5% D₂O with a final concentration of 70 μ M trimethylsilylpropanoic acid as an internal standard. Control spectrum was recorded under the same conditions without protein to confirm the absence of self-aggregated HR3744 or SAV13 macromolecules.

Molecular modelling

For molecular docking simulations, the SaeR structure from *S. aureus* (Protein Data Bank [PDB] entry 4qwq and 4ixa) was used. For preparation of the compounds and SaeR protein structures for docking, the three-dimensional structure of HR3744 was obtained with wincoot 0.8.1. Polar hydrogen atoms and Gasteiger charges were then added using autodock tools. Docking experiments with compound HR3744 were performed using a grid box covering the entire tetradecamer consisting of HR3744 chains A to B with a grid size of 40 \times 40 \times 60 and 1.0-Å resolution using Autodock vina software [45]. After docking, the conformation of the compound was analysed, and the (H bond and hydrophobic) interactions and three-dimensional models were generated with UCSF Chimera [46], LIGPLOT [47], or PyMol (Schrodinger LLC).

Mutagenesis

Thirty-one sets of primers were used to amplify the entire plasmid pRMC2-*saeR* for generating site-specific mutations. For example, for E159N, primer E159N-f and E159N-r was used for PCR amplification, with Phanta Max Super-Fidelity DNA Polymerase P505 (Vazyme, China). The resulting PCR products were purified using Purelink PCR purification kits and transformed to XL1-Blue competent *E. coli* cells. The mutated sequences of the *saeR* gene were verified and confirmed by DNA sequencing (BGI). Then,

plasmids were transformed into RN4220 competent cells and USA300- Δ saeR. Amino acid replaced SaeR proteins were expressed in USA300- Δ saeR for downstream gene expression by Western blot.

Mice bacteraemia infection models

BALB/c female mice of 6 to 8 weekold were housed in microisolator cages in a biosafety level 2 animal facility, and they received food and water ad libitum. A standard operating procedure was followed for the ethically approved protocols (CULATR 5439-20 and 5092-19) by committee on the use of live animals in teaching and research, the University of Hong Kong. The experiments were also conducted in biosafety level 2 animal facility. *S. aureus* strain USA300 was cultured to the early exponential phase of growth, washed twice with sterile phosphate-buffered saline solution (PBS), and resuspended in PBS at 1×10^7 CFU/100 μ L for the bacteraemia model and 5×10^7 CFU/100 μ L for the skin infection model.

The female Balb/c mice, 6–8 weeks old, were infected with *S. aureus* intravenously (i.v.) through the tail vein (200 μ L/ mouse) and randomized into three groups (8–10 mice per group). Another group with 10 mice received the same inoculum of *S. aureus* USA300- Δ saeR and this served as a control. One hour after infection, mice were treated with intraperitoneal injections of either the designated concentrations of compound HR3744 (7.5 mg/kg or 25 mg/kg) or compound SAV13 (4.9 mg/kg) or an injection of buffer (PBS with 2% DMSO and 2% Tween-80) which served as a vehicle. The compounds and injection buffer treatments were performed twice per day at 12-h intervals. On day 4, animals from each group were euthanized by overdose of dorminal (4%, 200 μ L/mouse via ip infection), their kidneys were harvested, homogenized in PBS, and plated on BHIA to obtain bacterial counts.

Subcutaneous infection model

For subcutaneous infection, the fur from the dorsal region of the mice was removed and infected with *S. aureus* USA300, USA300- Δ saeR, USA300- Δ saeS, USA300- Δ saeQRS, USA300- Δ agrA and USA300- Δ sigB at 5×10^7 via sub-cutaneous administration (100 μ L/mouse). The size of abscesses was monitored for 14 days. Then, the infected skin tissues were harvested, homogenized in PBS, and plated on LBA with clindamycin (1 μ g/mL) and erythromycin (1 μ g/mL) to obtain bacterial counts. The knockdown effect was determined by infecting the mice with USA300-pSD1 or USA300-pSD1saeR at 5×10^7 via sub-cutaneous administration with five mice per group. Six hours post infection, mice were treated with anhydrotetracycline (0.5 mg/kg) and

chloramphenicol (10 μ g/kg). The size of abscesses was monitored for 14 days. Animals from each group were euthanized by overdose of dorminal (4%, 200 μ L/mouse via ip infection) and bacterial loads from the abscess were determined by viable count.

Statistical analysis

All experiments were performed in triplicates unless specified otherwise. GraphPad Prism Software 8.0 was used for all statistical analyses. Results were presented as mean \pm SD. Specific statistical tests were indicated in the figure legends. * $P < .05$ was considered significant.

Acknowledgements

The authors also acknowledge the assistance of the University of Hong Kong Li Ka Shing Faculty of Medicine Faculty Core Facility. The sponsors had no role in the design and conduct of the study; in the collection, analysis, and interpretation of data; or in the preparation, review, or approval of the manuscript. We are grateful to Prof. Victor Torres, Prof. Taek Bae, Prof. Baolin Sun, Prof. Quanjiang Ji and Prof. Chia Lee for their generous gifts of plasmids pET41b-saeSc and pKOR1-saeQRS::spec, pET28b-saeR and pKOR1, pSD1, pCasSA and pCasSA-agrA, and pTL3801, pTL3685 and bacteriophage Φ 85, respectively.

Funding

This work was supported by Health and Medical Research Fund HMRP Project [grant number 19180692] to P. G., GRF project Research Grants Council, University Grants Committee [grant number 17104420] to R. Y. T. K. and R. G. C. of the Hong Kong SAR Project No. AoE/P-705/16 to R. Y. T. K. and RIF R7070-18 to HZ. S. and R. Y. T. K.








Author contributions

P. G. and R. K. conceived the work, designed the study, and wrote the manuscript. P. G. conducted all the experiments. Y. W., V. T., and P. G. did the gene deletion and animal experiments. H. L. and X. L. conducted the SAR analysis. P. L., K. S., and H. S. conducted the NMR waterLOGSY. S. H. and S. T. conducted the mutagenesis. S. H. and P. G. did the western blotting. J. C. supplied the clinical isolates. S. H. and P. H. P. contributed to drafting the manuscript. P. H. P. and R. K. supervised the study and helped interpretation of experimental results. All authors were involved in data analysis and assisted in editing the manuscript.

Disclosure statement

No potential conflict of interest was reported by the author(s).

ORCID

Peng Gao  <http://orcid.org/0000-0002-6877-6388>
 Han Liu  <http://orcid.org/0000-0003-1412-4584>
 Pradeep Halebeedu Prakash  <http://orcid.org/0000-0001-6124-5878>
 Kong-Hung Sze  <http://orcid.org/0000-0002-0898-605X>
 Jonathan Hon Kwan Chen  <http://orcid.org/0000-0002-7510-1696>
 Hongzhe Sun  <http://orcid.org/0000-0001-6697-6899>
 Xuechen Li  <http://orcid.org/0000-0001-5465-7727>
 Richard Yi-Tsun Kao  <http://orcid.org/0000-0001-8703-4980>

References

- [1] Cheung GYC, Bae JS, Otto M. Pathogenicity and virulence of *Staphylococcus aureus*. *Virulence*. 2021;12(1):547–569. doi:10.1080/21505594.2021.1878688
- [2] Kest H, Kaushik A. Vancomycin-resistant *Staphylococcus aureus*: formidable threat or silence before the storm. *J Infect Dis Epidemiol*. 2019;5(5):93–101. doi:10.23937/2474-3658/1510093
- [3] Siberry GK, Tekle T, Carroll K, et al. Failure of clindamycin treatment of methicillin-resistant *Staphylococcus aureus* expressing inducible clindamycin resistance in vitro. *Clin Infect Dis*. 2003;37(9):1257–1260. doi:10.1086/377501
- [4] Gao P, Wei Y, Wan RE, et al. Subinhibitory concentrations of antibiotics exacerbate staphylococcal infection by inducing bacterial virulence. *Microbiol Spectr*. 2022;10(4):e0064022. doi:10.1128/spectrum.00640-22
- [5] Rasko DA, Sperandio V. Anti-virulence strategies to combat bacteria-mediated disease. *Nat Rev Drug Discovery*. 2010;9(2):117–128. doi:10.1038/nrd3013
- [6] Dickey SW, Cheung GYC, Otto M. Different drugs for bad bugs: antivirulence strategies in the age of antibiotic resistance. *Nat Rev Drug Discov*. 2017;16(7):457–471. doi:10.1038/nrd.2017.23
- [7] Chihiro Sasakawa JH. Host-microbe interaction: bacteria. *Curr Opin Microbiol*. 2006;9(1):1–4. doi:10.1016/j.mib.2005.12.015
- [8] Sully EK, Malachowa N, Elmore BO, et al. Selective chemical inhibition of agr quorum sensing in *Staphylococcus aureus* promotes host defense with minimal impact on resistance. *PLoS Pathog*. 2014;10(6):e1004174. doi:10.1371/journal.ppat.1004174
- [9] Mellbye B, Schuster M. The sociomicrobiology of antivirulence drug resistance: a proof of concept. *mBio*. 2011;2(5):00131-11. doi:10.1128/mbio.00131-11
- [10] Goerke C, Fluckiger U, Steinhuber A, et al. Impact of the regulatory loci agr, sarA and sae of *Staphylococcus aureus* on the induction of alpha-toxin during device-related infection resolved by direct quantitative transcript analysis. *Mol Microbiol*. 2001;40(6):1439–1447. doi:10.1046/j.1365-2958.2001.02494.x
- [11] Giraudo AT, Calzolari A, Cataldi AA, et al. The sae locus of *Staphylococcus aureus* encodes a two-component regulatory system. *FEMS Microbiol Lett*. 1999;177(1):15–22. doi:10.1111/j.1574-6968.1999.tb13707.x
- [12] Sun F, Li C, Jeong D, et al. In the *Staphylococcus aureus* two-component system sae, the response regulator SaeR binds to a direct repeat sequence and DNA binding requires phosphorylation by the sensor kinase SaeS. *J Bacteriol*. 2010;192(8):2111–2127. doi:10.1128/JB.01524-09
- [13] Novick RP, Jiang D. The staphylococcal SaeRS system coordinates environmental signals with agr quorum sensing. *Microbiology*. 2003;149(Pt 10):2709–2717. doi:10.1099/mic.0.26575-0
- [14] Kuroda H, Kuroda M, Cui L, et al. Subinhibitory concentrations of beta-lactam induce haemolytic activity in *Staphylococcus aureus* through the SaeRS two-component system. *FEMS Microbiol Lett*. 2007;268(1):98–105. doi:10.1111/j.1574-6968.2006.00568.x
- [15] Jeong DW, Cho H, Lee H, et al. Identification of the P3 promoter and distinct roles of the two promoters of the SaeRS two-component system in *Staphylococcus aureus*. *J Bacteriol*. 2011;193(18):4672–4684. doi:10.1128/JB.00353-11
- [16] Liang X, Yu C, Sun J, et al. Inactivation of a two-component signal transduction system, SaeRS, eliminates adherence and attenuates virulence of *Staphylococcus aureus*. *Infect Immun*. 2006;74(8):4655–4665. doi:10.1128/IAI.00322-06
- [17] Zurek OW, Nygaard TK, Watkins RL, et al. The role of innate immunity in promoting SaeR/S-mediated virulence in *Staphylococcus aureus*. *J Innate Immun*. 2014;6(1):21–30. doi:10.1159/000351200
- [18] Liu Q, Cho H, Yeo WS, et al. The extracytoplasmic linker peptide of the sensor protein SaeS tunes the kinase activity required for staphylococcal virulence in response to host signals. *PLoS Pathog*. 2015;11(4):e1004799. doi:10.1371/journal.ppat.1004799
- [19] Borgogna TR, Hisey B, Heitmann E, et al. Secondary bacterial pneumonia by *Staphylococcus aureus* following influenza A infection is SaeR/S dependent. *J Infect Dis*. 2018;218(5):809–813. doi:10.1093/infdis/jiy210
- [20] Zhao C, Shu X, Sun B. Construction of a gene knock-down system based on catalytically inactive (dead) Cas9 (dCas9) in *Staphylococcus aureus*. *Appl Environ Microbiol*. 2017;83(12):e00291-17. doi:10.1128/AEM.00291-17
- [21] Cegelski L, Marshall GR, Eldridge GR, et al. The biology and future prospects of antivirulence therapies. *Nat Rev Microbiol*. 2008;6(1):17–27. doi:10.1038/nrmicro1818
- [22] Gordon CP, Williams P, Chan WC. Attenuating *Staphylococcus aureus* virulence gene regulation: a medicinal chemistry perspective. *J Med Chem*. 2013;56(4):1389–1404. doi:10.1021/jm3014635
- [23] Crossley KB. *Staphylococci in human disease*. 2nd ed. Chichester: Wiley-Blackwell; 2010.
- [24] Loffler B, Hussain M, Grundmeier M, et al. *Staphylococcus aureus* panton-valentine leukocidin is a very potent cytotoxic factor for human neutrophils. *PLoS Pathog*. 2010;6(1):e1000715. doi:10.1371/journal.ppat.1000715
- [25] Anderson MJ, Lin YC, Gillman AN, et al. Alpha-toxin promotes *Staphylococcus aureus* mucosal biofilm formation. *Front Cell Infect Microbiol*. 2012;2:64. doi:10.3389/fcimb.2012.00064
- [26] Schwartz K, Syed AK, Stephenson RE, et al. Functional amyloids composed of phenol soluble modulins stabilize *Staphylococcus aureus* biofilms. *PLoS Pathog*. 2012;8(6):e1002744. doi:10.1371/journal.ppat.1002744
- [27] Cheng AG, Kim HK, Burts ML, et al. Genetic requirements for *Staphylococcus aureus* abscess formation and persistence in host tissues. *FASEB J*. 2009;23(10):3393–3404. doi:10.1096/fj.09-135467
- [28] Voyich JM, Vuong C, DeWald M, et al. The SaeR/S gene regulatory system is essential for innate immune

- evasion by *Staphylococcus aureus*. *J Infect Dis*. 2009;199(11):1698–1706. doi:10.1086/598967
- [29] Flack CE, Zurek OW, Meishery DD, et al. Differential regulation of staphylococcal virulence by the sensor kinase SaeS in response to neutrophil-derived stimuli. *Proc Natl Acad Sci U S A*. 2014;111(19):E2037–E2045.
- [30] Jeong DW, Cho H, Lee H, et al. Identification of the P3 promoter and distinct roles of the two promoters of the SaeRS two-component system in *Staphylococcus aureus*. *J Bacteriol*. 2011;193(18):4672–4684. doi:10.1128/JB.00353-11
- [31] Mainiero M, Goerke C, Geiger T, et al. Differential target gene activation by the *Staphylococcus aureus* two-component system saeRS. *J Bacteriol*. 2010;192(3):613–623. doi:10.1128/JB.01242-09
- [32] Gao P, Wang YL, Villanueva I, et al. Construction of a multiplex promoter reporter platform to monitor staphylococcus aureus virulence gene expression and the identification of Usnic acid as a potent suppressor of psm gene expression. *Front Microbiol*. 2016;7:1344. doi:10.3389/fmicb.2016.01344
- [33] Gao P, Ho PL, Yan B, et al. Suppression of *Staphylococcus aureus* virulence by a small-molecule compound. *Proc Natl Acad Sci USA*. 2018;115(31):8003–8008. doi:10.1073/pnas.1720520115
- [34] Malachowa N, DeLeo FR. *Staphylococcus aureus* survival in human blood. *Virulence*. 2011;2(6):567–569. doi:10.4161/viru.2.6.17732
- [35] [van] Wamel WJ, Rooijackers SH, Ruyken M, et al. The innate immune modulators staphylococcal complement inhibitor and chemotaxis inhibitory protein of *Staphylococcus aureus* are located on beta-hemolysin-converting bacteriophages. *J Bacteriol*. 2006;188(4):1310–1315. doi:10.1128/JB.188.4.1310-1315.2006
- [36] Pietrocola G, Nobile G, Rindi S, et al. *Staphylococcus aureus* manipulates innate immunity through own and host-expressed proteases. *Front Cell Infect Microbiol*. 2017;7:166. doi:10.3389/fcimb.2017.00166
- [37] Zhou C, Bhinderwala F, Lehman MK, et al. Urease is an essential component of the acid response network of *Staphylococcus aureus* and is required for a persistent murine kidney infection. *PLoS Pathog*. 2019;15(1):e1007538. doi:10.1371/journal.ppat.1007538
- [38] Methicillin-resistant *Staphylococcus aureus* (MRSA) protocols. Totowa (NJ): Humana Press; 2007 (Ji Y, editor).
- [39] Ohlsen K, Ziebuhr W, Koller KP, et al. Effects of sub-inhibitory concentrations of antibiotics on alpha-toxin (hla) gene expression of methicillin-sensitive and methicillin-resistant *Staphylococcus aureus* isolates. *Antimicrob Agents Chemother*. 1998;42(11):2817–2823. doi:10.1128/AAC.42.11.2817
- [40] Bae T, Schneewind O. Allelic replacement in *Staphylococcus aureus* with inducible counter-selection. *Plasmid*. 2006;55(1):58–63. doi:10.1016/j.plasmid.2005.05.005
- [41] Niesen FH, Berglund H, Vedadi M. The use of differential scanning fluorimetry to detect ligand interactions that promote protein stability. *Nat Protoc*. 2007;2(9):2212–2221. doi:10.1038/nprot.2007.321
- [42] Hong SW, Choi EB, Min TK, et al. An important role of alpha-hemolysin in extracellular vesicles on the development of atopic dermatitis induced by *Staphylococcus aureus*. *PLoS One*. 2014;9(7):e100499. doi:10.1371/journal.pone.0100499
- [43] Petit L, Gibert M, Gillet D, et al. Clostridium perfringens epsilon-toxin acts on MDCK cells by forming a large membrane complex. *J Bacteriol*. 1997;179(20):6480–6487. doi:10.1128/jb.179.20.6480-6487.1997
- [44] Yuan S, Chu H, Huang J, et al. Viruses harness YxxO motif to interact with host AP2M1 for replication: a vulnerable broad-spectrum antiviral target. *Sci Adv*. 2020;6(35):eaba7910, doi:10.1126/sciadv.aba7910
- [45] Trott O, Olson AJ. Autodock vina: improving the speed and accuracy of docking with a new scoring function, efficient optimization, and multithreading. *J Comput Chem*. 2010;31(2):455–461.
- [46] Pettersen EF, Goddard TD, Huang CC, et al. UCSF chimera – a visualization system for exploratory research and analysis. *J Comput Chem*. 2004;25(13):1605–1612. doi:10.1002/jcc.20084
- [47] Wallace AC, Laskowski RA, Thornton JM. LIGPLOT: a program to generate schematic diagrams of protein-ligand interactions. *Protein Eng*. 1995;8(2):127–134. doi:10.1093/protein/8.2.127